BIOCHEMISTRY
including biophysical chemistry & molecular biology
Article

Biochemistry **2009,** *48,* 11161–11168 11161
DOI: 10.1021/bi9010122

The Mechanistic Architecture of Thermostable *Pyrococcus furiosus* Family B DNA Polymerase Motif A and Its Interaction with the dNTP Substrate†

Edward M. Kennedy, Christopher Hergott, Stephen Dewhurst, and Baek Kim*

Department of Microbiology and Immunology, University of Rochester Medical Center, Rochester, New York 14642

Received June 16, 2009; Revised Manuscript Received September 22, 2009

ABSTRACT: Thermostable DNA polymerases isolated from archaeal organisms have not been completely characterized kinetically and require further study if we are to understand both their dNTP binding mechanism and their role within the organism. Here, we demonstrate that the thermostable family B DNA polymerase from *Pyrococcus furiosus* (Pfu Pol) contains sensitive determinants of both dNTP binding and replicational fidelity within the highly conserved motif A. Site-directed mutagenesis of the motif A SYLP region revealed that small shifts in side chain volume result in significant changes in the dNTP binding affinity, steady state kinetics, and fidelity of the enzyme. Mutants of Y410 show high fidelity in both misincorporation assays and forward mutation assays, but display a substantially higher K_m than the wild type. In contrast, mutations of upstream residue L409 result in a drastically reduced affinity for the correct dNTP, a much higher efficiency of both misincorporation and mismatch extension, and substantially lower fidelity as demonstrated by a PCR-based forward mutation assay. The A408S mutant, however, displayed a significant increase in both dNTP binding affinity and fidelity. In summary, these data show that modulation of motif A can greatly shift both the steady and pre-steady state kinetics of the enzyme as well as the fidelity of Pfu Pol.

DNA polymerases, which are conserved throughout Archaea, Bacteria, and Eukarya, are responsible for replication and maintenance of their respective organism's genomes. These polymerases have been organized into broad families by sequence similarity, and most DNA polymerases responsible for chromosomal replication are grouped into families B and C, with prominent examples being the eukaryotic δ- and ε-polymerases and *Escherichia coli* polymerase III α subunit, respectively (*1*). Family B also contains many virus, phage, and archaeal DNA polymerases, including the well-studied RB69 gp43 polymerase (*2*).

Many archaeal DNA polymerases from hyperthermophilic organisms, which are uniquely capable of synthesizing DNA at extremely high temperatures, have been isolated but have yet to be studied in mechanistic detail. In addition to *Thermus aquaticus* polymerase (Taq Pol) (*3*), several thermostable archaeal Y family DNA polymerases such as the DinB homologue (Dbh) and DNA polymerase IV (dpo4), thought to be involved in DNA repair, have been kinetically characterized (*4*, *5*). The thermostable B family polymerase Vent polymerase has been characterized for its ability to incorporate nucleotide analogues (*6*), but a detailed study of dNTP binding, kinetics, and replicational fidelity of this and other thermostable B family polymerases remains to be conducted.

The thermostable Pfu DNA polymerase (Pfu Pol) is an archaeal family B or human pol α-like DNA polymerase isolated from *Pyrococcus furiosus* (*7*). Pfu Pol has superior fidelity compared to thermostable Taq DNA polymerase because of 3′ to 5′ proofreading exonuclease activity (*8*). Pfu Pol, like other family B DNA polymerases, contains the conserved domains motif A and motif C. These domains form the core molecular surface of the active site in the palm domain and coordinate the two metal ions necessary for catalysis (*9*). Specifically, motif A contains two of the aspartate residues that participate in coordination of these metals, and it also contains a central SLYP motif that is solvent exposed in the prototypical RB69 gp43 polymerase. In crystal structures of RB69 gp43 polymerase and HIV-1 reverse transcriptase (RT) containing both template/primer (T/P) and substrate, the side chain of the motif A tyrosine (SLYP) has been shown to stack with the ribose of the incoming dNTP (Figure 1A). This residue is also known to participate in substrate selection and is thought to sterically clash with the rNTP 2′-OH group. This prevents incorporation of rNTPs by both DNA-dependent and RNA-dependent DNA polymerases such as Φ29, RB69 gp43, Vent, and MuLV RT (*10*−*13*). Similarly, Pfu Pol motif A contains Y410, which is analogous to the well-studied aromatic residues described above. In this work, we have experimentally tested the hypothesis that this amino acid of Pfu Pol motif A and its surrounding residues may be essential for optimal dNTP binding affinity and replicational fidelity via modification of the conserved central tyrosine and its surrounding residues. The results of this analysis provide an understanding of the role of motif A in dNTP binding, discrimination, and incorporation in a thermostable family B polymerase.

EXPERIMENTAL PROCEDURES

Construction of Pfu Pol Mutants. Overlap extension polymerase chain reaction (PCR) was used to generate mutant Pfu Pol exonuclease-inactive (D215A) derivatives, which were then

†This research was supported by Grant CA122213 (B.K. and S.D.), Grant DOD W81XWH-07-10376 (B.K. and S.D.), and Training Grant T32 AI007362 (E.M.K.) from the National Institutes of Health.

*To whom correspondence should be addressed: Department of Microbiology and Immunology, University of Rochester Medical Center, 601 Elmwood Ave., Box 672, Rochester, NY 14642. Telephone: (585) 275-6916. E-mail: baek_kim@urmc.Rochester.edu.

Published on Web 10/09/2009

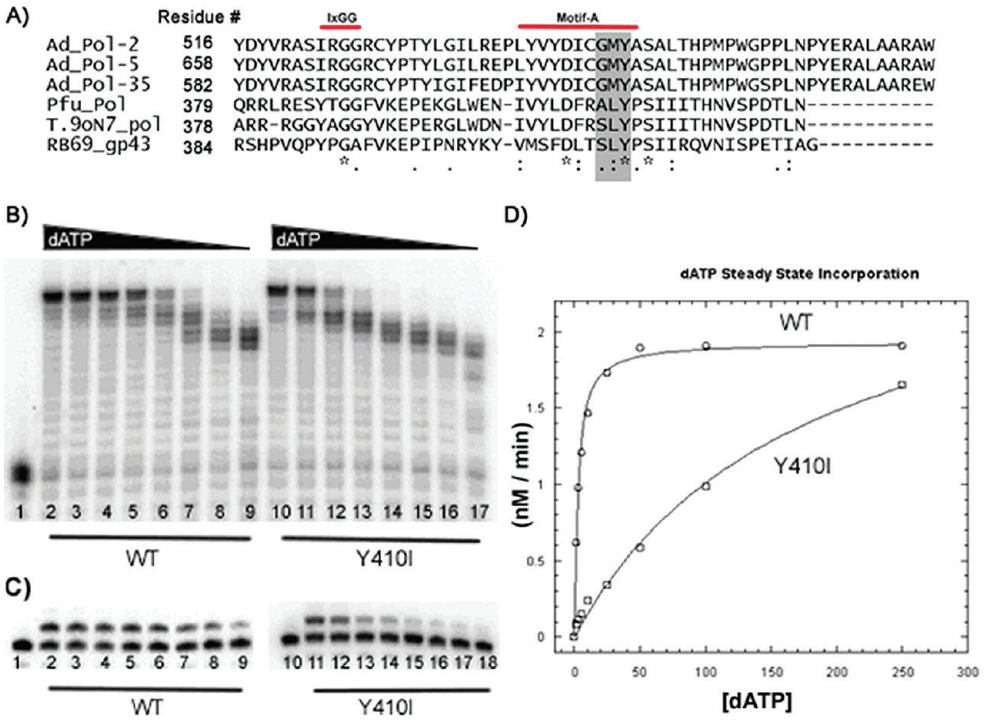

FIGURE 1: PFU steady state kinetics and dNTP utilization. (A) Clustal-W multisequence alignment of adenovirus (serotypes 2, 5, and 35), Pfu Pol, *Thermococcus* species 9oN7° Pol, and RB69 gp43 phage polymerase motif A. The specific area of interest to this study is highlighted in gray. Asterisks denote identical residues, colons conserved substitutions, and periods semiconserved substitutions. (B) Multiple nucleotide incorporation reactions were conducted with a 5′ end ^{32}P-labeled 23-mer primer annealed to a 40-mer DNA template at 55 °C for 5 min with varying amounts of all four dNTPs. No enzyme control (lane 1) indicates the position of the 23-mer unextended primer. A representative multinucleotide dNTP titration for wild-type (WT) Pfu Pol 3′−5′ exo$^-$ (lanes 2−9) and Pfu Pol mutant Y410I (lanes 10−17) is shown; concentrations of dNTP for each set of eight reactions were 250, 100, 50, 25, 10, 5, 2.5, and 1 μM. (C) Representative single-nucleotide (dATP) titrations for WT Pfu Pol (lanes 2−9) and Y410I (lanes 11−18) conducted at 55 °C as described for panel B, except using only dATP. (D) Nonlinear regression fit of the Michaelis−Menten equation to the single-nucleotide extension performed in duplicate for WT (○) and Y410I (□).

inserted into pET28a plasmids (Novagen) for bacterial expression. The motif A mutations were then created by PCR-based site-directed mutagenesis.

Purification of Pfu Pol. Pfu Pol proteins were overexpressed in *E. coli* BL21 pLysS (Invitrogen) from pET28a plasmids containing the Pfu Pol genes, which are fused to six histidine residues at their N-terminal ends. Following lysis and centrifugation, the hexahistidine-tagged polymerases were purified using Ni^{2+} chelation chromatography as described previously (*14*−*16*). Following two dialysis steps in Pfu dialysis buffer [50% glycerol and 50 mM Tris-HCl (pH 8.8)], the protein was compared to 0.5−4 μg of 98% pure bovine serum albumin (BSA) (Bio-Rad) by 10% sodium dodecyl sulfate−polyacrylamide gel electrophoresis (SDS−PAGE) and Coomassie blue staining. This analysis was used to estimate protein concentration (at ∼2 mg/L of protein of interest) to approximate protein purity (which was similar to that of 98% pure BSA).

Steady State Kinetic Assays. The DNA 40-mer template was annealed to 23-mer ^{32}P 5′ end-labeled primer as described previously (*15*). 20nM of the template/primer complex (T/P) was extended with Pfu Pol in the following conditions for all reactions at 55 °C for 5 min and quenched with stop dye (10 μL of 40 mM EDTA, 99% formamide) and incubated for 5 min at 95 °C. First, protein dilution reactions were conducted with 250 μM dATP to normalize the activities of the Pfu Pol proteins displaying ∼50% extension (equal fully extend and unextended products) in single dATP extension reactions. Then, these protein concentrations displaying the 50% primer extension were used for subsequent dATP (Amersham Biosciences) single nucleotide extension titrations at defined substrate concentrations 250, 100, 50, 25, 10, 5, 2.5, and 1 μM. The Michaelis−Menten constant was obtained from nonlinear regression fit of the Michaelis−Menten equation, and values obtained were subsequently verified with Lineweaver−Burk double-reciprocal plots.

Pre-Steady State Kinetic Assays. First, single-turnover burst assays were performed to assess the active site concentrations of WT and mutant Pfu Pol proteins on a 5′ end ^{32}P-labeled DNA 23-mer annealed to the DNA 40-mer. TTP (800 μM) was mixed rapidly with 100 nM Pfu Pol protein precomplexed with 100 nM ^{32}P-labeled T/P and 200 nM cold T/P in a rapid quencher (Kintek RFQ3). Subsequent quenching with 0.5 M EDTA at a set range of time points was then performed, and the product formation at each time point was analyzed and fitted to eq 1, which determined the active site concentration of each Pfu Pol protein. Second, the pre-steady state reactions with 200 nM active protein and 100 nM T/P were performed to assess the observed rates of product formation (k_{obs}) at six or seven time points in duplicate per dTTP concentration. The k_{obs} values were then fitted to eq 2 as described below to yield K_d and k_{pol}.

Data Analysis. For the pre-steady state assays, data were curve-fitted with nonlinear regression to eqs 1 and 2 with KaleidaGraph as described previously (*17*, *18*).

$$[\text{product}] = A[1 - \exp(-k_{obs}t) + k_{ss}t] \quad (1)$$

Equation 1 was used to obtain the amplitude of the burst (A) from a burst assay time course. This allowed calculation of the percentage of active Pfu Pol molecules in an individual protein preparation. Resulting k_{obs} values from dNTP titration

experiments were then fitted with eq 2 to yield K_d and k_{pol}.

$$k_{obs} = k_{pol}[dNTP]/(K_d + [dNTP]) \quad (2)$$

PCR-Based lacZα Forward Mutation Assay. Both WT exo$^+$ and exo$^-$ and mutant thermostable Pfu Pol (all exo$^-$), purified as described above, were diluted serially to determine the optimal protein concentration for inverse PCR of the entire pUC18 (3218 bp) DNA via analysis of the reaction product on a 0.7% agarose gel. These concentrations were then used in a 100 μL PCR with a starting template of *Afl*III-linearized pUC18 at a concentration of 50 ng. These reactions were sampled every five cycles, and the copy number was subsequently determined after a 10^6-fold dilution via QT-PCR with the TaqMan probe (5′-TAM-TCTTCCGCTTCCTCGCTCACTGA-FAM-3′) with the amplification oligomers: 5′-AGAGGCGGTTTGCGTATT-3′ and 5′-TGTTCTTTCCTGCGTTATCC-3′. The PCRs were then terminated at the cycles giving very similar copy numbers of the amplified products by the Pfu Pol proteins. These amplified entire pUC18 DNA products were purified via a Qiagen column, digested with *Bgl*II, ligated and transformed via electroporation into α-complemented *E. coli* strain XL-1 blue (Stratagene), and plated on IPTG, carbenicillin, and Xgal containing 2×-YT agar plates. Note that the *Bgl*II restriction site lies in the nonessential region of pUC18. Blue (wild-type) and white/pale blue (mutant) colonies were then counted at a sample size greater than 500 for the entire experiment; this analysis was performed in triplicate for each Pfu Pol derivative. This entire procedure was also performed with no enzyme, and the value obtained was subtracted from values obtained for the Pfu Pol derivatives. Though the white/blue value obtained for the experiment without enzyme ranged from 0.09 to 0.11, which was higher than expected, it was consistent throughout all experiments and was substantially lower than any values obtained for Pfu Pol experiments. The mutant colonies from the reactions with WT and L409M proteins were also randomly selected for sequencing, and these were then compared to an overall consensus to determine the mutational spectrum. Few or no founder mutations were evident in subsequent alignments of sequenced mutants, indicating that template doublings were effectively minimized and mutations above background were indeed due to mutation synthesis during DNA synthesis.

Terminal Transferase Assay. A 19-mer DNA template annealed to an 18-mer 5′ end ^{32}P-labeled DNA primer was prepared as previously described (*19*). Reactions were completed with dATP or dCTP at 250 μM with an equal activity under the conditions described above.

Visualization and Quantification of Biochemical Assays. All reactions completed in the steady or presteady state with Pfu Pol were processed similarly. Four microliters of the final reaction products were quantified by phosphorimaging analysis (PerkinElmer Life Sciences) of 16% acrylamide−urea denaturing gels (SequaGel, National Diagnostics; model S2 sequencing gel electrophoresis apparatus, Labrepco). Signal was quantified with Optiquant or Quailty One (Bio-Rad) via comparison of the amount of extended product to the total signal per reaction.

RESULTS

Kinetic Analysis of Pfu Pol Motif A Mutants. The central "steric gate" tyrosine (Tyr) or phenylalanine (Phe) in well-conserved motif A is responsible for the selective utilization of dNTP versus rNTP substrates by many Pol α family polymerases and reverse transcriptases. This Tyr or Phe residue is presumed to sterically clash with the rNTP 2′-OH group and likely participates in a van der Waals stacking interaction with the sugar moiety of the incoming dNTP substrate. To investigate the role of the corresponding residue in the functional activity of the Pfu DNA polymerase, we performed site-directed mutagenesis on the Tyr 410 (Y410) residue of Pfu DNA polymerase and its two preceding residues, L409 and A408. To minimize the gross structural effects of these substitutions, we mutated these targeted residues of motif A to amino acids with physicochemical characteristics similar to those of the wild-type residues. We therefore created the following mutants: Y410L, Y410I, Y410V, L409I, L409V, L409M, L409F, and A408S. Initially, we employed a steady state kinetic screening assay at 55 °C to evaluate the overall impact of the motif A mutations on the dNTP concentration-dependent product formation in the polymerase background without 3′−5′ exonuclease activity (D215A substitution). Subsequent pre-steady state kinetic analysis and steady state fidelity assays were then performed with Pfu Pol WT and select mutants to investigate the specific effects of motif A mutations.

Table 1: Motif A Mutant Steady State Kinetic Parameters at 55 °C

Pfu Pol[a]	K_m (μM)	k_{cat} (s^{-1})	k_{cat}/K_m (μM^{-1} s^{-1})
WT	2.5 ± 0.3	0.022 ± 0.003	0.009
Y410L	69 ± 16	0.31 ± 0.043	0.004
Y410I	130 ± 7.3	0.32 ± 0.03	0.002
Y410V	46 ± 7.7	0.029 ± 0.006	0.001
L409I	14 ± 6.5	0.022 ± 0.001	0.002
L409M	2.0 ± 0.4	0.028 ± 0.001	0.014
L409V	12 ± 0.4	0.034 ± 0.006	0.003
A408S	10 ± 1.2	0.037 ± 0.001	0.004

[a]All with the 3′−5′ exonuclease inactive D215A mutation.

First, in both steady state single- and multiple-nucleotide incorporation analyses, we observed that mutations at residues 410, 409, and 408 altered incorporation kinetics. Y410I displayed the most significant reductions in dNTP concentration-dependent activity among the mutants tested in both multiple-incorporation (Figure 1B) and single-incorporation (Figure 1C) reactions. Quantifying the products of a similar single-nucleotide extension reaction and fitting them to the Michaelis−Menten equation allowed us to obtain K_m and k_{cat} (Figure 1D and Table 1). Although steady state kinetic assays do not reveal the specific mechanistic effects resulting from active site mutations, they are useful for screening many mutants and may indicate overall enzyme function or dysfunction (i.e., they report the sum of the entire deoxynucleotide incorporation equilibrium reviewed in ref *20*). Comparison of Pfu Pol WT exo$^-$ to Y410 mutants revealed a profound defect in dNTP utilization at lower substrate concentrations in both multiple-nucleotide and single-nucleotide extension. We observed a 20−61-fold difference in K_m when comparing WT to the Y410 mutants, representing the largest kinetic defect. Mutation of the L409 residue resulted in a more subtle steady state defect relative to WT, with an approximate 5-fold difference between the WT enzyme versus L409I or L409V (Table 1). Possibly, alterations of Y410 itself or the neighboring side chains to a less bulky hydrophobic residue reduce or shift the molecular surface available for a van der Waals interaction with the ribose moiety of an incoming dNTP. In contrast, a conservative substitution of the A408 residue with serine had little effect on steady state kinetic parameters (reflected by only a slight

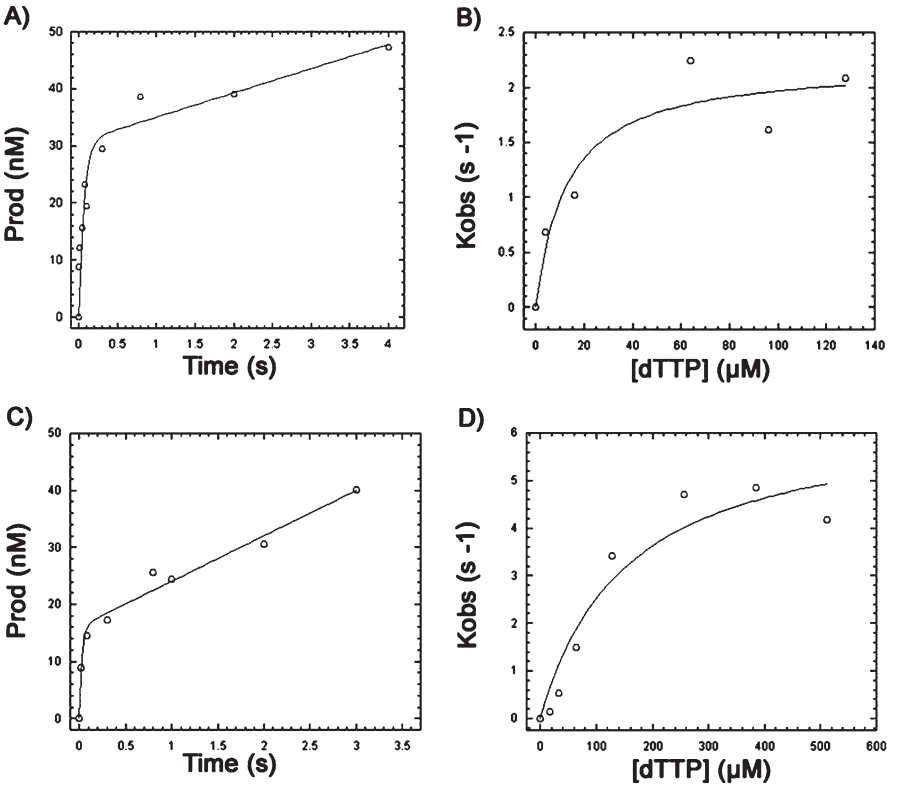

FIGURE 2: Pre-steady state active site titrations and dNTP titration curves for WT and L409M. The burst kinetic study was conducted in duplicate for all mutants as well as WT Pol at 37 °C; the mean product formation per time was used to assess the occurrence of the burst, and the activate site concentrations were determined with eq 1. Template/primer (T/P) was used in 3-fold excess of the enzyme, allowing both pre-steady state and steady state incorporation to be examined. (A) WT Pfu Pol active site titration. This preparation was 29% active. (B) WT Pfu Pol pre-steady state dNTP titration using 100 nM active protein with 25 nM T/P. (C) L409M active site titration. This preparation was 20% active. (D) L409M pre-steady state dNTP titration using 100 nM active protein with 25 nM T/P.

reduction in K_m), although it did result in increased affinity for the incoming dNTP as measured by the pre-steady state kinetics (see below and Table 1). We also constructed and examined additional residue A408 mutants (G, C, and V) and surprisingly found that these mutants either had grossly impaired activity or were completely inactive (data not shown) in contrast to the more conservative A408S mutant (Table 1). This demonstrates that A408 plays an important structural role in the function of the motif A loop and is essential for polymerase function.

Pre-Steady State Kinetics of Pfu Pol Motif A Mutants. Steady state kinetics can indicate general changes in enzyme function, but to fully understand Pfu Pol kinetics, we conducted pre-steady state quench flow analysis. To further characterize the mechanistic alterations made by the Pfu Pol Motif A mutants, we chose WT and three mutants, A408S, L409M, and Y410V, and performed pre-steady state analysis of incorporation of the template cognate nucleotide (dTTP). First, we determined the active site concentration of each of the Pfu Pol proteins in burst reactions (panels A and C of Figure 2 for WT and L409M, respectively). We observed approximately 20−60% activity among the Pfu Pol proteins. Next, a single-round pre-steady state dTTP titration for each protein was performed (panels B and D of Figure 2 for WT and L409M, respectively). Similar to the trend observed in the steady state assays, we observed a decrease in binding affinity for all mutants involving residues 409 and 410 (Table 2). Indeed, both L409M and Y410V mutants had a higher K_d than WT, with the defect exhibited by L409M being most substantial at 21-fold (Table 2). Our pre-steady state analyses indicate that very small side chain volume shifts in the Pfu Pol motif A residues can significantly alter not only the dNTP affinity but also its maximum rate of conformational change and catalysis (k_{pol}).

Table 2: Motif A Mutant Pre-Steady State Kinetic Parameters at 37 °C

Pfu Pol[a]	K_d (μM)[b]	k_{pol} (s^{-1})	k_{pol}/K_d
WT	14 ± 2.8	2.2 ± 0.01	0.15
Y410V	38 ± 27 (3×)	3.7 ± 0.4	0.10
L409M	310 ± 8.5 (22×)	9.8 ± 1.2	0.03
A408S	4.4 ± 2.1	1.9 ± 0.1	0.42

[a]All with the 3′−5′ exonuclease inactive D215A mutation. [b]Reactions were performed at 37 °C.

Impact of Motif A Mutations on Pfu Pol Fidelity. Next, we investigated whether motif A mutations also affect enzyme fidelity. First, we established a new PCR-based *lac*Zα forward mutation assay. In this assay, the entire pUC18 plasmid was amplified to an equivalent extent by each of the Pfu Pol protein mutants, as determined by quantitative PCR (see Experimental Procedures). The amplified linear pUC18 DNAs were then digested, ligated, and transformed to XL-1 Blue *E. coli* host cells, and the cells were plated on IPTG/X-gal agar. The numbers of mutant (pale blue and white) colonies and wild-type (dark blue) colonies were counted and used to determine the mutant rate for each Pfu Pol protein. As a test of this assay system, we performed control reactions using WT Pfu Pol with and without 3′ to 5′ proofreading exonuclease activity. As shown in Figure 3, we observed that exo$^+$ Pfu Pol exhibited a 26-fold lower mutation frequency than exo$^-$ Pfu Pol. The extent of this fidelity difference is comparable with the fold difference previously reported in reversion-based mutation assays, thus validating our PCR-based

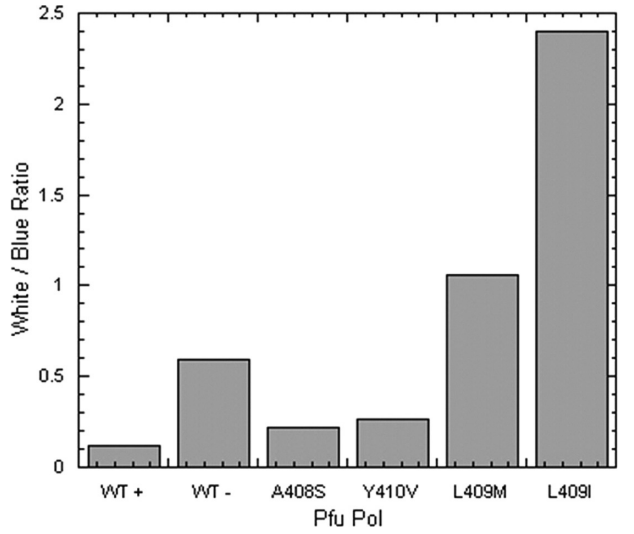

FIGURE 3: Mutant frequencies of Pfu DNA polymerase motif A mutants. The mean ratios of pale blue and white to blue colonies (gray bars) are displayed for the *lac*Zα forward mutation assay performed in triplicate as described in Experimental Procedures. The columns display data for WT+ (WT Pfu Pol with 3′−5′ exonuclease), WT− (Pfu Pol without the exonuclease), A408S, Y410V, L409M, and L409I (note that all mutant enzymes were 3′−5′ exonuclease deficient, unless otherwise indicated). A no enzyme control was performed to assess the background frequency of the *lac*Zα mutation; these background values were subtracted from the values calculated for each of the Pfu DNA polymerase motif A mutants. Results shown represent mean mutant frequencies, and standard deviations are as follows: 0.026 for WT+, 0.063 for WT−, 0.049 for A408S, 0.081 for Y410V, 0.292 for L409M, and 1.362 for L409I.

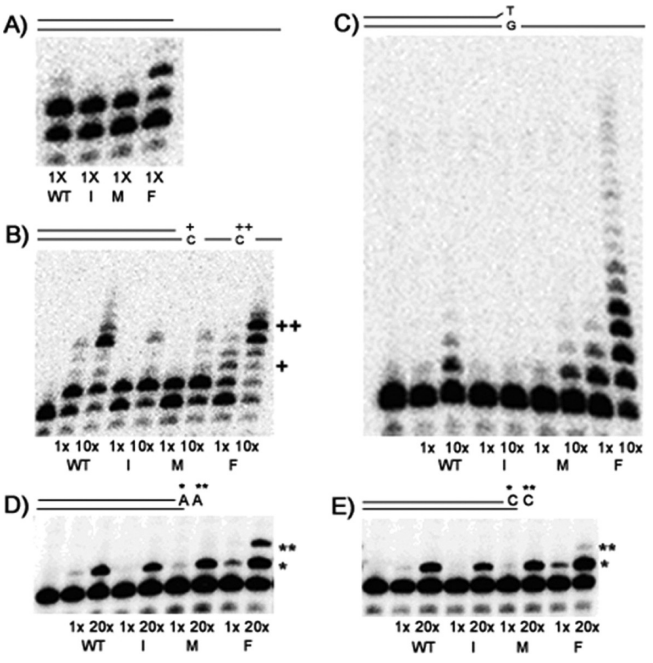

FIGURE 4: L409 mutant misinsertion, mismatch extension, and TNTase activity. (A) Reactions were first conducted with matched template/primer and 250 μM dTTP at 55 °C to demonstrate that equal activity (1×) was used for each Pfu Pol protein (I for L409I, M for L409M, and F for L409F). (B) Matched template/primer was used in a misincorporation assay with two equal activities (1× and 10×) of each Pfu Pol protein and only three dNTPs (dATP, dCTP, and dTTP) at 250 μM without dGTP. Shown are the sites of the first (+) and second (++) templated cytosines. (C) Extension of a G/T mismatched T/P by WT and L409 mutants in the presence of four dNTPs at 250 μM. (D) Extension of a 18-mer/19-mer T/P (T templated) by two equal activities and (20×) by Pfu Pol WT and L409 mutants in the presence of 250 μM dATP. One asterisk denotes the first dATP incorporation; two asterisks denote the second untemplated dATP incorporation. (E) Extension of a 18-mer/9-mer T/P (G templated) by two equal activities (1× and 20×) by Pfu Pol WT and L409 mutants in the presence of 250 μM dCTP.

fidelity assay (*8*). Next, we determined the mutation rate of four motif A mutants, Y410V, A408S, L409M, and L409I. As shown in Figure 3, the Y410V and A408S mutants exhibited slightly lower mutation rates than WT exo$^-$ Pfu Pol, whereas the two L409 mutant proteins exhibited an increased mutation frequency.

Next, we employed primer extension-based polymerase fidelity assays that monitor misinsertion and mismatch extension, which are two key steps involved in the synthesis of a single mutation during the enzymatic DNA polymerization reaction. First, we normalized the input activity for our WT and L409 mutant polymerases (Figure 4A); we then performed multiple-nucleotide primer extension reactions in the presence of only three dNTPs (dATP, dTTP, and dCTP). Under biased dNTP pool conditions such as these, polymerization pauses one nucleotide before sites where the missing dNTP (dGTP in this case) should be incorporated; these pause sites are commonly termed stop sites (see the intense bands immediately before the + in Figure 4B). Low-fidelity polymerases tend to add incorrect dNTPs at stop sites and thus generate a higher level of primer extension product following a stop site. Indeed, the L409F Pfu Pol mutant exhibited larger amounts of primer extension beyond the stop sites, indicating that it is a low-fidelity Pfu mutant.

We also simulated the second step of mutation synthesis, mismatch extension, by performing a similar primer extension reaction using a mismatched primer and all four dNTPs (Figure 4C). In this reaction, the L409F mutant displayed extensive mismatch extension activity. It is important to note that this mutant obligatorily appends additional nucleotides, even at very low levels of input activity (panels C and A of Figure 4, respectively). Taken together, both the PCR-based forward *lac*Zα mutation assay and the gel-based fidelity assays confirmed that mutations of the L409 residue lower the fidelity of Pfu Pol. Interestingly, similar steady state characterization of mutants of the analogous residue (L868) in human polymerase α also showed an enhanced ability to bypass aberrant DNA lesions and a higher error frequency than WT, as shown by both reversion and forward mutation assays (*21*).

Untemplated Nucleotide Addition Activity of Pfu L409F Mutants. From the data discussed above, the L409 residue appears to be essential for maintaining the fidelity of Pfu Pol. Pfu Pol L409F exhibits the highest efficiency of misincorporation and mismatch extension in the qualitative gel extension assays (Figure 4), even though this mutant was unable to complete a PCR under the conditions used in our forward mutation assay described below. To further analyze the low fidelity of the L409F mutant, we tested whether this mutant was able to polymerize DNA in the absence of the template. This test was based on the notion that low-fidelity enzymes may incorporate dNTPs even in the absence of proper base pairing with template nucleotides and/or without the need for the enzyme active site to be occupied by a template DNA.

For this test, we employed a 5′ end-labeled 18-mer primer annealed to 19-mer templates, generating 5′ end single-nucleotide overhangs (T for Figure 4C and G for Figure 4D). These 18-mer/19-mer T/Ps were incubated with an equal amount of active polymerase [WT and L409F proteins (see Figure 4A)]. As shown

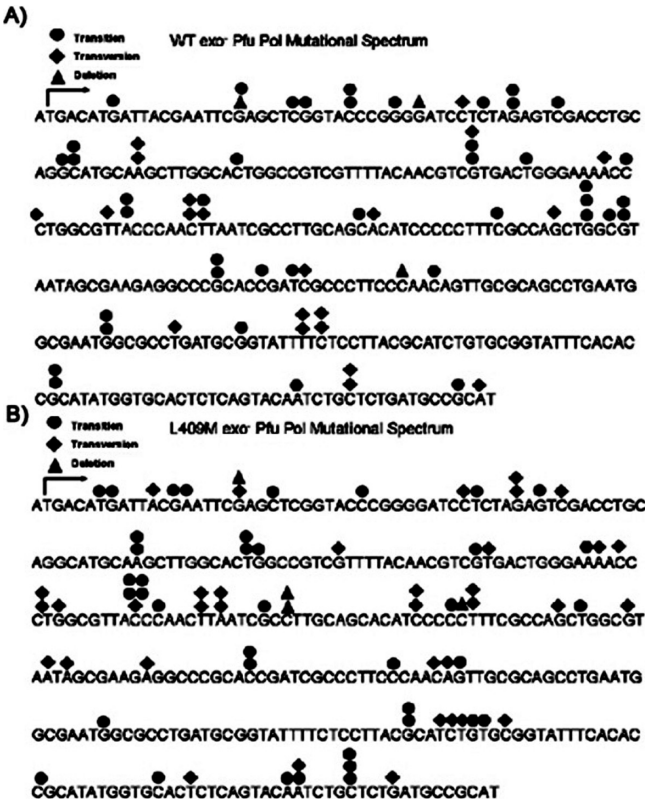

FIGURE 5: WT (A) and L409M (B) Pfu Pol mutational spectrum. The types of mutations produced by WT or L409M exo$^-$ polymerases are overlaid upon the *lac*Zα sequence for WT (A) and L409M (B).

in the reactions with dATP (Figure 4C) or dCTP (Figure 4D), L409F was able to incorporate a second untemplated dATP or dCTP, whereas the WT enzyme did not show any significant incorporation of an untemplated dNTP. This ability to incorporate a second dATP or dCTP could be due to primer/template slippage. However, we designed a template sequence that is unlikely to form slippage intermediates (see Experimental Procedures). Thus, we conclude that the L409F mutant displays high untemplated dNTP incorporation capability, which is mechanistically similar to the incorporation of mispaired or unpaired dNTPs.

Mutation Spectrum Effect of the L409 Mutant. Finally, we tested whether the error-prone L409 mutants produce a distinct mutational spectrum when compared to WT Pfu DNA polymerase. For this test, we selected mutant colonies from the PCR-based forward mutation assay for the WT and L409 mutants and sequenced the *lac*Zα region of the plasmid recovered from the mutant colonies. The L409F mutant was a logical choice for this analysis because of its profound effect on enzyme fidelity in our other assays. However, this mutant was insufficiently active to generate a PCR product in our novel lacZ forward mutation assay. We therefore selected the L409M mutant for analysis. As shown in Table 2, the L409M mutant exhibited more transversions and fewer transitions than WT exo$^-$. Similar active site architecture changes have been shown to produce equivalent mutator phenotypes, with a bias toward transversion, in thermostable Taq Pol (*22*). In addition, the WT and L409M polymerases exhibited significantly different mutational hot spots (Figure 5), indicating that the L409M mutation affects the mutation spectrum specificity as well as the mutation frequency as summarized in Figure 3.

DISCUSSION

We present here a detailed kinetic characterization of Pfu Pol, which provides a more complete understanding of the interaction of a thermostable DNA polymerase with its dNTP substrate. These studies shed light on the role of the conserved motif A in Pfu Pol, which not only is informative from a biochemical perspective, but also may aid in the development of therapeutics targeting related viral DNA polymerases that are insoluble or otherwise difficult to study or characterize (i.e., adenovirus DNA polymerase). Moreover, the details of thermostable Pfu Pol kinetics and fidelity are of interest both to the biotechnology community and to those studying the archaeal DNA replication machinery.

As indicated by both steady state and pre-steady state kinetics, conservative substitutions of the Y410 residue in motif A of the polymerase impact the affinity of the enzyme for its substrate, suggesting that the Pfu polymerase likely interacts with the incoming dNTP in a manner similar to that of other family B polymerases (*10*, *12*, *13*). Subtle shifts in residue L409 adjacent to Y410 produce drastic changes in Pfu Pol fidelity, assessed both biochemically and by the newly established PCR-based forward mutation assay. Interestingly, among the conservative L409 mutants that we studied, L409M may be unique, as demonstrated by the subtle defect in K_m and the drastic defect in K_d when compared to WT. The relatively higher k_{pol} and possibly a faster overall product release step may compensate for the low relative affinity of L409M for the incoming dNTP, though this requires further study.

Pfu Pol can serve as a tractable model for insoluble or otherwise recalcitrant α-like viral polymerases that may be medically or therapeutically important. We therefore conducted our reactions at 37 °C to assess dNTP binding at a biologically relevant temperature. Thermostable enzymes are thought to be more rigid than mesophilic ones and are known to function poorly at mesophilic ranges from 20 to 37 °C (reviewed in ref *23*). Comparison of mesophilic to thermostable adenylate kinase revealed a lower turnover number at low temperatures because of a slower rate of conformational change required for catalysis to occur (*24*).

DNA polymerases have previously been shown to undergo substantial dNTP binding conformational change before catalysis, and Pfu Pol may be similarly impacted at mesophilic temperatures. When compared to those of Vent polymerase and RB69 gp43 polymerase, the amplitude of our burst occurs at a later time point (100 ms), which can easily be explained by our suboptimal reaction temperature of 37 °C relative to the optimal temperature of 72 °C. Similarly, Pfu Pol k_{pol} values are likely lower than their maximal value because of the reaction temperature. Overall temperature-dependent differences in kinetic parameters are intriguing and indicate there are substantial differences in function at higher optimal temperatures. We did not measure K_d or the dissociation constant of Pfu Pol for the dsDNA template/primer which to our knowledge has not been measured; temperature may also impact it. However, the final concentration of T/P in our burst assays (300 nM) is well above the K_d values reported for *Thermus aquaticus* DNA polymerase (10 nM), RB69 gp43 DNA polymerase (< 100 nM), and T4 DNA polymerase (70 nM), and Pfu Pol is likely saturated (*3*, *25*, *26*). Furthermore, we have observed an increase in percent activity (measured by active site titration) with temperature of at least 2-fold for reactions conducted at 30 °C versus 60 °C

(data not shown) which indicates that template/primer binding improves with temperature. Both template/primer binding and dNTP incorporation may shift under high-temperature conditions due to the high diffusion rate and an increase in the rate of conformational change, and collectively, this may explain the low activity observed in our burst assays conducted at 37 °C.

The kinetics of selection of dNTP versus rNTP substrates has been well characterized for both family A (e.g., Klenow fragment) and family B DNA polymerases such as Vent, Φ29, and RB69, and both MuLV and HIV-1 reverse transcriptases (*10*−*13*, *27*, *28*). Exclusion of rNTPs by Klenow fragment is mediated by residue E710 and the nearby F762 residue, through a presumed direct steric clash with the incoming nucleotide 2′-OH group. In family B DNA polymerases, a similar effect is mediated by a single Tyr residue which is functionally analogous to these Klenow residues (*29*). Specifically, it has been suggested that a central tyrosine ring may sterically clash with the 2′-OH group of the rNTP substrate, and it has been shown that mutations that disrupt this moiety permit an enhanced steady state incorporation of rNTPs (*10*, *12*, *30*). Although no pre-steady state kinetics have been determined for similar mutants of reverse transcriptases, MuLV RT exhibits a slight decrease in K_m with the F155V substitution (*11*).

Both Φ29 (Y254) and Vent (Y412) polymerases have a subtle steady state defect upon permutation of the conserved central Y to V, L, or F (*10*, *12*). More interesting, however, is the pre-steady state characterization of the Y416A and Y416F mutants of RB69 polymerase. The Y416A substitution yields a K_d (dNTP) similar to that of WT, relative to the 3-fold increase shown by Y416F (*13*). This implies that the hydroxyl moiety may play a role in the ring orientation that is favorable for binding and that Y416A, though greatly decreasing the K_d for the rNTP substrate, does not impact the affinity of polymerase for dNTPs. Thus, the bulky hydrophobic side chains (I, V, and L) used to replace the key tyrosine (Y410) in this study of Pfu Pol are likely in a distinct conformation relative to the WT Tyr residue. These mutations may disrupt the WT molecular surface and reduce dNTP binding affinity in a fashion similar to that of Y416F in RB69 polymerase. Kinetic properties of family B polymerases containing mutants at L409 or analogous residues have not been previously reported in the literature, although a mutator phenotype similar to that identified in this study in Pfu Pol has been documented in *Saccharomyces cerevisiae* DNA polymerase α; this directly supports both our forward mutation and biochemical assay data (*21*). Overall, L409 mutants with increasing side chain volume have successively more drastic fidelity defects, culminating with L409F, which is misincorporated with exceptional efficiency. This suggests that L409 participates architecturally in overall polymerase function with respect to base selection, and that its replacement with large hydrophobic side chains may bias the active site toward misincorporation over incorporation.

In conclusion, our results clearly demonstrate that motif A contains crucial determinants of WT fidelity (L409) and that conservative modification of specific residues can directly affect dNTP binding kinetics and fidelity.

ACKNOWLEDGMENT

We thank Erin Noble for helpful suggestions.

REFERENCES

1. Ito, J., and Braithwaite, D. K. (1991) Compilation and alignment of DNA polymerase sequences. *Nucleic Acids Res. 19*, 4045–4057.
2. Braithwaite, D. K., and Ito, J. (1993) Compilation, alignment, and phylogenetic relationships of DNA polymerases. *Nucleic Acids Res. 21*, 787–802.
3. Brandis, J. W., Edwards, S. G., and Johnson, K. A. (1996) Slow rate of phosphodiester bond formation accounts for the strong bias that Taq DNA polymerase shows against 2′,3′-dideoxynucleotide terminators. *Biochemistry 35*, 2189–2200.
4. Fiala, K. A., and Suo, Z. (2004) Pre-steady-state kinetic studies of the fidelity of *Sulfolobus solfataricus* P2 DNA polymerase IV. *Biochemistry 43*, 2106–2115.
5. Cramer, J., and Restle, T. (2005) Pre-steady-state kinetic characterization of the DinB homologue DNA polymerase of *Sulfolobus solfataricus*. *J. Biol. Chem. 280*, 40552–40558.
6. Gardner, A. F., Joyce, C. M., and Jack, W. E. (2004) Comparative kinetics of nucleotide analog incorporation by vent DNA polymerase. *J. Biol. Chem. 279*, 11834–11842.
7. Uemori, T., Ishino, Y., Toh, H., Asada, K., and Kato, I. (1993) Organization and nucleotide sequence of the DNA polymerase gene from the archaeon *Pyrococcus furiosus*. *Nucleic Acids Res. 21*, 259–265.
8. Cline, J., Braman, J. C., and Hogrefe, H. H. (1996) PCR fidelity of pfu DNA polymerase and other thermostable DNA polymerases. *Nucleic Acids Res. 24*, 3546–3551.
9. Sousa, R. (1996) Structural and mechanistic relationships between nucleic acid polymerases. *Trends Biochem. Sci. 21*, 186–190.
10. Bonnin, A., Lazaro, J. M., Blanco, L., and Salas, M. (1999) A single tyrosine prevents insertion of ribonucleotides in the eukaryotic-type phi29 DNA polymerase. *J. Mol. Biol. 290*, 241–251.
11. Gao, G., Orlova, M., Georgiadis, M. M., Hendrickson, W. A., and Goff, S. P. (1997) Conferring RNA polymerase activity to a DNA polymerase: A single residue in reverse transcriptase controls substrate selection. *Proc. Natl. Acad. Sci. U.S.A. 94*, 407–411.
12. Gardner, A. F., and Jack, W. E. (1999) Determinants of nucleotide sugar recognition in an archaeon DNA polymerase. *Nucleic Acids Res. 27*, 2545–2553.
13. Yang, G., Franklin, M., Li, J., Lin, T. C., and Konigsberg, W. (2002) A conserved Tyr residue is required for sugar selectivity in a Pol α DNA polymerase. *Biochemistry 41*, 10256–10261.
14. Weiss, K. K., Isaacs, S. J., Tran, N. H., Adman, E. T., and Kim, B. (2000) Molecular architecture of the mutagenic active site of human immunodeficiency virus type 1 reverse transcriptase: Roles of the β8-αE loop in fidelity, processivity, and substrate interactions. *Biochemistry 39*, 10684–10694.
15. Malboeuf, C. M., Isaacs, S. J., Tran, N. H., and Kim, B. (2001) Thermal effects on reverse transcription: Improvement of accuracy and processivity in cDNA synthesis. *BioTechniques 30*, 1074–1078, 1080, 1082.
16. Kim, B. (1997) Genetic selection in *Escherichia coli* for active human immunodeficiency virus reverse transcriptase mutants. *Methods 12*, 318–324.
17. Skasko, M., Weiss, K. K., Reynolds, H. M., Jamburuthugoda, V., Lee, K., and Kim, B. (2005) Mechanistic differences in RNA-dependent DNA polymerization and fidelity between murine leukemia virus and HIV-1 reverse transcriptases. *J. Biol. Chem. 280*, 12190–12200.
18. Weiss, K. K., Chen, R., Skasko, M., Reynolds, H. M., Lee, K., Bambara, R. A., Mansky, L. M., and Kim, B. (2004) A role for dNTP binding of human immunodeficiency virus type 1 reverse transcriptase in viral mutagenesis. *Biochemistry 43*, 4490–4500.
19. Diamond, T. L., Roshal, M., Jamburuthugoda, V. K., Reynolds, H. M., Merriam, A. R., Lee, K. Y., Balakrishnan, M., Bambara, R. A., Planelles, V., Dewhurst, S., and Kim, B. (2004) Macrophage tropism of HIV-1 depends on efficient cellular dNTP utilization by reverse transcriptase. *J. Biol. Chem. 279*, 51545–51553.
20. Joyce, C. M., and Benkovic, S. J. (2004) DNA polymerase fidelity: Kinetics, structure, and checkpoints. *Biochemistry 43*, 14317–14324.
21. Niimi, A., Limsirichaikul, S., Yoshida, S., Iwai, S., Masutani, C., Hanaoka, F., Kool, E. T., Nishiyama, Y., and Suzuki, M. (2004) Palm mutants in DNA polymerases α and η alter DNA replication fidelity and translesion activity. *Mol. Cell. Biol. 24*, 2734–2746.
22. Suzuki, M., Yoshida, S., Adman, E. T., Blank, A., and Loeb, L. A. (2000) *Thermus aquaticus* DNA polymerase I mutants with altered fidelity. Interacting mutations in the O-helix. *J. Biol. Chem. 275*, 32728–32735.
23. Vieille, C., and Zeikus, G. J. (2001) Hyperthermophilic enzymes: Sources, uses, and molecular mechanisms for thermostability. *Microbiol. Mol. Biol. Rev. 65*, 1–43.

24. Wolf-Watz, M., Thai, V., Henzler-Wildman, K., Hadjipavlou, G., Eisenmesser, E. Z., and Kern, D. (2004) Linkage between dynamics and catalysis in a thermophilic-mesophilic enzyme pair. *Nat. Struct. Mol. Biol. 11*, 945–949.
25. Capson, T. L., Peliska, J. A., Kaboord, B. F., Frey, M. W., Lively, C., Dahlberg, M., and Benkovic, S. J. (1992) Kinetic characterization of the polymerase and exonuclease activities of the gene 43 protein of bacteriophage T4. *Biochemistry 31*, 10984–10994.
26. Zhang, H., Cao, W., Zakharova, E., Konigsberg, W., and De La Cruz, E. M. (2007) Fluorescence of 2-aminopurine reveals rapid conformational changes in the RB69 DNA polymerase-primer/template complexes upon binding and incorporation of matched deoxynucleoside triphosphates. *Nucleic Acids Res. 35*, 6052–6062.
27. Astatke, M., Grindley, N. D., and Joyce, C. M. (1998) How *E. coli* DNA polymerase I (Klenow fragment) distinguishes between deoxy- and dideoxynucleotides. *J. Mol. Biol. 278*, 147–165.
28. Boyer, P. L., Sarafianos, S. G., Arnold, E., and Hughes, S. H. (2000) Analysis of mutations at positions 115 and 116 in the dNTP binding site of HIV-1 reverse transcriptase. *Proc. Natl. Acad. Sci. U.S.A. 97*, 3056–3061.
29. Astatke, M., Ng, K., Grindley, N. D., and Joyce, C. M. (1998) A single side chain prevents *Escherichia coli* DNA polymerase I (Klenow fragment) from incorporating ribonucleotides. *Proc. Natl. Acad. Sci. U.S.A. 95*, 3402–3407.
30. Yang, G., Franklin, M., Li, J., Lin, T. C., and Konigsberg, W. (2002) A conserved Tyr residue is required for sugar selectivity in a Pol α DNA polymerase. *Biochemistry 41*, 2526–2534.